X International Conference on Computational Methods in Marine Engineering
MARINE 2023
J. Garcia-Espinosa, L. González, J.E. Gutiérrez & B. Serván-Camas (Editors)

Full-Scale CFD simulations of Air Lubrication with DIS-Based Air Cavity for Planing Hull

MARINE 2023

Fabio De Luca[1], Simone Mancini[1]*, Claudio Pensa[1], Riccardo Pigazzini[1], Vincenzo Sorrentino[1,2]

[1] Università degli Studi di Napoli "Federico II", Dipartimento di Ingegneria Industriale

[2] EURISCO Consulting SRL

[*] Corresponding author: Simone Mancini, simone.mancini@unina.it

ABSTRACT

The air lubrication system represents among the others one of the most promising solutions in the maritime industry to reduce fuel consumption and carbon emissions. However, this energy-saving solution is usually applied on displacement hulls where simulations, tests, and trials have been largely investigated. The application of air lubrication systems on planing or semi-planing hulls is indeed not common, as those hulls are characterized by a different hydrodynamic behavior that can influence the effectiveness of the air lubrication solution. In addition, full-scale analyses of this energy-saving technology are in general rather rare, in particular for its application on planing hulls. The current investigation is part of a wide experimental and numerical research campaign that aims to analyze the application of an air injection system where the air cavity is obtained by a DIS (Double Interceptor System) installed on the bottom of a planing hull. The aim of the present study is to provide an insight into the potential scale effects of an air injection system combined with the DIS system on a planing hull through Computational Fluid Dynamics (CFD) simulations and how scale effects could impact the full-scale efficiency of this energy-saving technology application. The CFD simulations of the planing hull with DIS and air injection system have been carried out in model and full-scale. Model scale results are then compared against towing tank model tests.

Keywords: planing hull; air lubrication; air cavity; Double Interceptor (DIS); Full-scale CFD.

NOMENCLATURE

AL	Air Lubrication
ACDR	Air Cavity Drag Reduction
ALDR	Layer Drag Reduction
BDR	Bubble Drag Reduction
CFD	Computational Fluid Dynamics
CG	Center of Gravity
DIS	Double Interceptor System
HSMV	High-Speed Marine Vehicles
λ	Scale ratio
VOF	Volume of Fluid
Q_{nm}	Model Scale Natural Ventilation Air Flow Rate (kg/s)
$2Q_{nm}$	2x Model Scale Natural Ventilation Air Flow Rate (kg/s)
$5Q_{nm}$	5x Model Scale Natural Ventilation Air Flow Rate (kg/s)
Q_{fs}	Scaled Natural Ventilation Air Flow Rate (kg/s)
$2Q_{fs}$	2x Scaled Natural Ventilation Air Flow Rate (kg/s)
$5Q_{fs}$	5x Scaled Natural Ventilation Air Flow Rate (kg/s)
Q_{ns}	Full Scale Natural Ventilation Air Flow Rate (kg/s)

1. INTRODUCTION

In recent years, the sustainability and environmental impact of maritime transport is one of the main concerns among multiple national and international (MEPC 2013) maritime authorities. As a result, both the maritime research community as well as shipyards, and the maritime industry in general are working towards the construction of more efficient vessels. An increase in efficiency has two major implications, the first is a reduced cost of exercise for the owner, more so in the light of increasing fuel prices and second it benefits the environment by reducing emissions. From the marine engineer's perspective, the efforts focus on more efficient power production and reducing exhaust gas emissions. From the naval architecture perspective, the main goal is to reduce the ship's total resistance.

Among the various resistance reduction methods for ships, one of the most promising technologies is Air Lubrication (AL). A detailed overview of the research progress of AL can be found in An *et al*. (2022). Three main typologies of Air Lubrication can be identified, Bubble Drag Reduction (BDR), Air Layer Drag Reduction (ALDR), Air Cavity Drag Reduction (ACDR), each one differs according to the amount of air flow rate and the way it is injected beneath the hull bottom. In BDR mode, at a relatively small flow rate, the air in the form of micro-bubbles is injected into the turbulent boundary layer. As the flow rate increases the micro-bubbles merge into a continuous air layer and a transitional phase from BDR to ALDR can be observed. In ACDR the air is injected in a hull cavity specifically designed to form an interface of air and water inside the hull cavity. To avoid air leakage from the sides and keep the cavity in pressure, the ACDR requires a large amount of air flow rates compared to ALDR and BDR.

The effectiveness and the applicability of AL strongly depend on the hull form. A deeply immersed flat bottom hull or a well-designed cavity is optimal for an air lubrication system, due to the better diffusion of the air layer and the air containment ability of a hull cavity. Therefore, most of the produced research has focused on flat plates in water tunnels and large bottom ship models in towing tanks. Regarding air lubrication for high-speed craft, the most studied technology is the ACDR. A historical description of the first applications of AL for high-speed craft can be found in Latorre (1997), the author conducted a systematic study on the performances of various high-speed catamarans and monohulls with bottom air injection highlighting the improvements in terms of speed increase and the dependence of the airflow rate on the resistance reduction anticipating the existence of an airflow threshold above that no significative resistance reduction can be seen. A resistance reduction of up to 20% was obtained by Gökçay *et al.* (2004), by means of an air cavity form in a planing hull. The increase of air flow did not lead to further drag reduction, but rather kept the cavity filled with air and in pressure. Later the data obtained in the experimental campaign were used for validating a CFD study with a VOF model for the description of the air-water interface (Gökçay and Insel, 2011). Cucinotta *et al.* (2017) analyzed the effect of the air injection on a planing hull equipped with different shapes of shallow step cavities, with the intention of developing an air layer instead of an air-cushion. Recently, Ricks *et al.* (2023) tested a stepped planing hull with a ventilated cavity.

An important aspect of AL is the correlation of the model scale test data to full scale, to evaluate the applicability of this technology and estimate the net savings. It is important to conduct large scale experiments and establish how far away from the air injection location the friction resistance reduction can be observed. Based on BDR experiments on a 50 meter flat plate, Kodama *et al.* (2000) observed a maximum resistance reduction of 23% at 7 m/s and a minor resistance reduction with higher speed. The Authors proposed an example of the application of the AL to a 300 m tanker, assuming the same friction resistance reduction of the 50 m flat plate. Regarding air cavity ships, Foeth *et al.* (2008) made an extrapolation assuming an equal wave resistance coefficient between the air-lubricated ship and full wetted one and a negligible cavity form drag. The recommended procedure adopted for full scale performance prediction, when AL techniques are applied, is described in ITTC Recommended Procedure 7.5-02-02-03, Resistance and Propulsion Test and Performance Prediction with Skin Frictional Drag Reduction Techniques.

In previous work by De Luca *et al.* (2022), an air lubrication solution for a planing hull that combines the air lubrication technique in conjunction with an air cavity provided by a DIS is presented through CFD simulations

and comparison with towing tank data. The effects of air lubrication on the performance of the hull have been evaluated through a systematic variation in the airflow rate and hull speed. The results showed a drag reduction of up to 16% compared to the DIS-only case due to the wetted surface reduction provided by the dry patch's increased size behind the forward interceptor. CFD results of increasing air flow rates show that at higher speeds the reduction in total resistance does not necessarily follow the increase of injected airflow. In order to evaluate the feasibility of the DIS-based air cavity concept, in the present work full scale effects are investigated using CFD simulations.

The aim of the present work is the study of the application of air lubrication on a DIS equipped planing hull, with a focus on scaling effects. The results of the experimental runs performed by De Luca *et al*. (2022) with natural ventilation air flow (Q_{nm}) have been used as the benchmark for CFD simulations in model scale. The study of the scale effects of air lubrication has been conducted by investigating three main aspects:

- The study of a scaling method of the air flow rate assuming Froude's scaling law for the velocity of the air flow.
- The applicability of the common full scale extrapolation ITTC procedure for High-Speed Marine Vehicles (ITTC 2017), merging experimental and CFD data.
- The analysis of the scale effects of a variable air flow rate, comparing the model scale and full scale performance improvements.

2. Numerical and experimental setup

The CFD simulations for this study have been carried out using the commercial CFD code Siemens PLM Star CCM+. The unsteady RANS simulations implement the Overset/Chimera mesh with a linear interpolation scheme between the background and the overset grids to allow hull motions (details by De Luca *et al.* (2016)). The segregated flow is solved using the Semi-Implicit Method for Pressure-Linked Equations (SIMPLE) algorithm for the pressure-velocity coupling, together with the Algebraic Multi-Grid (AMG) solver for faster convergence. The free surface was modeled with the two-phase Volume of Fluid (VOF) approach, with a High-Resolution Interface Capturing (HRIC) scheme based on the Compressive Interface Capturing Scheme for Arbitrary Mesh (CICSAM). The hybrid *All Wall y+* approach for the wall treatment has been implemented, for details regarding this approach see Siemens PLM Star-CCM+ v 2021.2 User's Guide (Siemens, 2021). The computational domain dimensions and the boundary conditions applied are depicted in Fig. 1. The domain dimensions comply with ITTC guidelines (ITTC, 2014) and the time step adopted. The forced airflow rate was determined by setting a given value at the mass flow outlet boundary (Figure 1). For the cases in which the performance of natural ventilation was evaluated, the resulting natural mass flow, Q_{nm} and Q_{ns}, was measured at the mass flow pipe outlets without any artificial mass flow condition being imposed. The flow outlets under the hull were open to atmospheric pressure, modeling the geometry of the pipes.

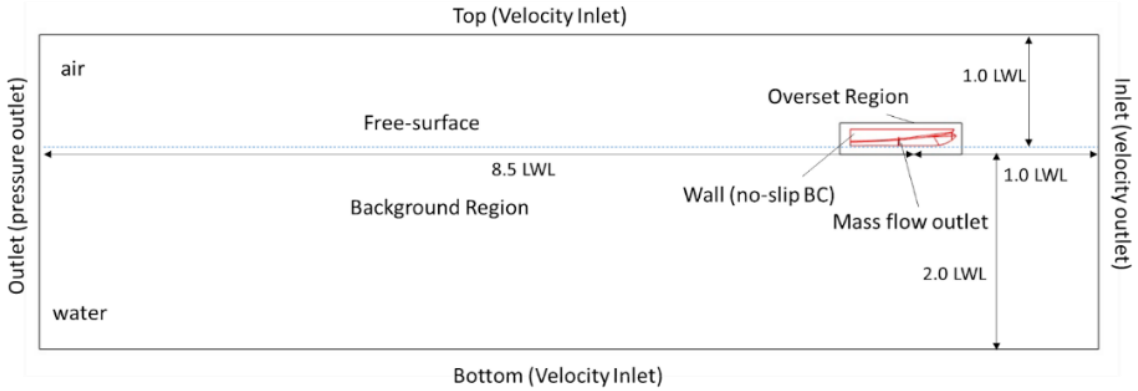

Figure 1. Computational domain and boundary conditions

Experiments were carried out at the LEIN towing tank at the Università degli Studi di Napoli "Federico II". The experimental restraints were set up to provide free trim and pitch through a cardan joint at the hull CG, together with vertical guides at the bow and aft to restrain yaw motion. Due to the high speed involved (Re > 1.0×10^7) in the test together with the presence of the DIS, no turbulence stimulators were used for the experiments. The model's mass configuration (see Table 1) used for the experiments led to a static trim of 0.6° forward.

Fig. 2 shows the benchmark hull considered in this study with a zoom-in view of the DIS and the air injection pipes. In Tab. 1 the principal dimensions are listed. A detailed description of the functionality of the DIS can be found in De Luca and Pensa (2012).

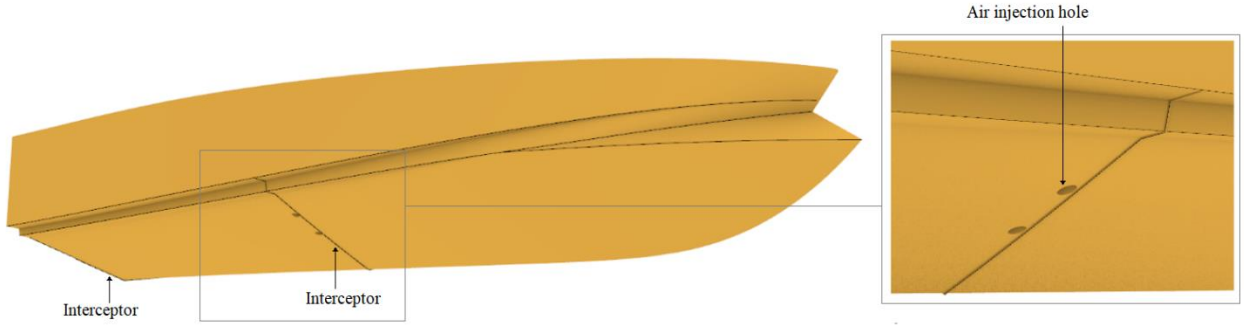

Figure 2. Hull equipped with DIS, with details on the air injection device.

Table 1. C1505 Model, model and full-scale hull details.

Dimension	Model Scale	Full scale
LWL (m)	2.313	11.565
BWL (m)	0.909	4.545
T (m)	0.157	0.785
LCB (m)	0.867	4.335
∇ (m3)	0.110	13.776

3. RESULTS AND DISCUSSION

Recalling previous work on the topic (De Luca 2022), the comparison between Towing Tank and CFD results in natural ventilation is proposed in Figures 3a and 3b in terms of resistance and trim. Percentage differences were evaluated with the ratio of CFD to experimental data.

Fig. 3a shows small differences in resistance, less than 2.5%. Conversely, Figure 3b shows minimal differences between the absolute values for the highest speeds and a large difference between the experimental and numerical values obtained at 4.6 m/s. The data analysis must be carried out in relation to the substantial coincidence of the resistances at this speed. This apparent inconsistency can possibly be explained by the fact that the ventilation of the aft area of the bow interceptor was not obtained in the Towing Tank, yet was achieved through numerical simulation. This circumstance caused a significant difference in trim, which, in turn, affected the drag in two opposite ways. In regard to the experimentation, the lower trim resulted in an increase

in the wetted surface and frictional resistance, as well as a decrease in pressure resistance due to the lower values of dynamic trim.

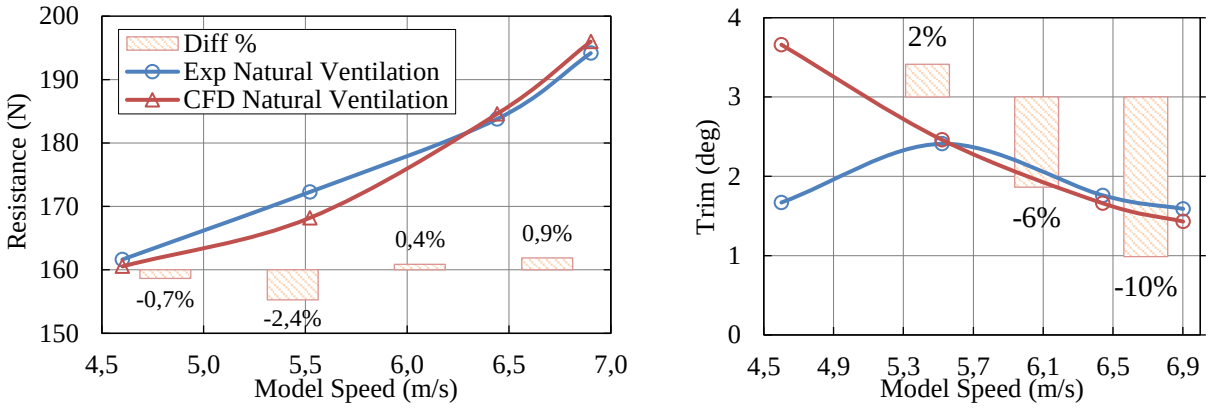

Figure 3. Comparison between model scale experimental and CFD results, in natural ventilation $\boldsymbol{Q_{nm}}$.

3.1 Air flow rate scaling

The proposed approach is based on the hypothesis that the model scale air flow velocity v_{air_M} in natural ventilation mode, can be scaled as the free stream velocity, *i.e.* the hull speed. Therefore, with the law:

$$v_{air_S} = \sqrt{\lambda} v_{air_M} \tag{1}$$

Where v_{air_M} is calculated knowing the air flow rate Q_{nm} and the geometry of the pipes. Hence, since the pipe section area is scaled by λ^2, the full scale air flow rate is scaled by the law:

$$Q_{fs} = \lambda^{5/2} Q_{nm} \tag{2}$$

Now, in order to evaluate the scaling approach of Eq. 2, the scaled air flow rate is compared with the natural flow rate Q_{ns} obtained by full scale CFD simulations. The results are shown in Fig. 6, where the differences are calculated with respect Q_{ns}. The plot shows that the scaled flow rate Q_{fs} is consistently higher than the actual measured flow rate Q_{ns} and the difference increases with speed. This observation leads to the conclusion that the actual scale factor exponent is lower than 2.5, as suggested in Eq. 2.

To properly evaluate the scaling law, knowing Q_{ns} and Q_{nm} from the CFD simulations, an estimation of the actual exponent for λ for scaling the air flow rate could be made:

$$x = log_{\lambda} \frac{Q_{ns}}{Q_{nm}} \tag{3}$$

Where x is the flow rate scale factor exponent estimated by a linear regression of $Q_{nm} - Q_{ns}$ curve obtained from CFD simulations at different Froude numbers. The resulting exponent is $x = 2.4$, therefore the new full scale air flow rate, for this specific case, can be calculated as:

$$Q_{fsx} = \lambda^{2.4} Q_{nm} \tag{4}$$

The plot in Fig. 4 shows the curves of Q_{ns}, Q_{fs}, Q_{fsx} and the differences in percentage to the full scale natural flow rate Q_{ns}. The new scaled air flow rate Q_{fsx} is closer to Q_{ns} curve than Q_{fs}, with a maximum difference of 7.4% at Fr 0.97. Therefore, the scaling law $\lambda^{2.4}$ is a better approximation for scaling the natural air flow rate Q_{nm}.

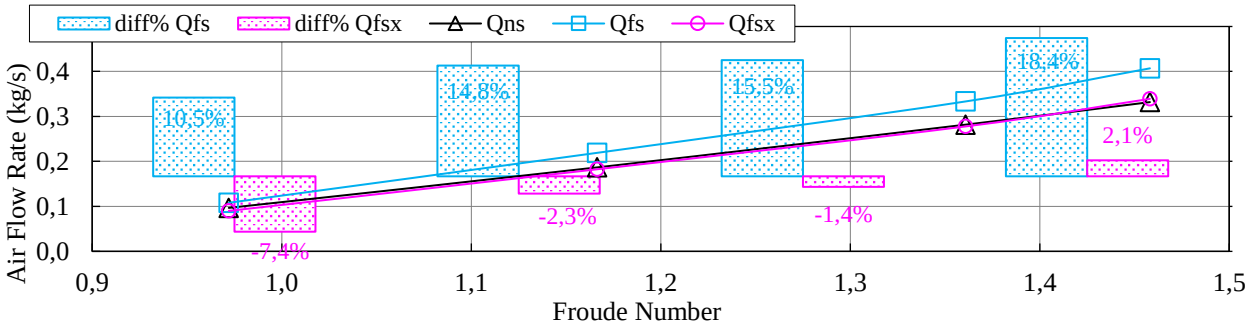

Figure 4. Comparison between $\boldsymbol{Q_{ns}}$ (black curve), $\boldsymbol{Q_{fs}}$ (cyan curve) and $\boldsymbol{Q_{fsx}}$ (magenta curve). The differences are calculated respect to $\boldsymbol{Q_{ns}}$.

3.2 Resistance scaling

Regarding the resistance extrapolation, the ITTC procedure for High-Speed Marine Vehicles Resistance Test (ITTC 2017) has been applied. In the following data reduction equations:

$$C_R = C_{TM} - C_{FM}\frac{S_M}{S_{0M}} \tag{5}$$

$$C_{TS} = C_R + C_{FS}\frac{S_S}{S_{0S}} \tag{6}$$

it has been assumed the hypothesis of an equal wetted surface ratio in model scale and in full scale:

$$\frac{S_M}{S_{0M}} = \frac{S_S}{S_{0S}} \tag{7}$$

Where, S_M is the model scale running wetted surface area calculated from CFD simulations, S_{0M} is the model scale nominal wetted surface area, calculated at zero speed. Likewise for the full scale wetted surface area, scaled by the factor λ^2. This scaling assumes that the residuary resistance is not affected by the presence of the air injection and an equal wetted surface reduction effect is present in both model scale and full scale.

The results of the proposed scaling approach in terms of resistance curves, trim, and rise of CG are reported in Fig. 5 (a) and (b). The curve resulting from the resistance correlation approach is the cyan-square curve (ITTC), and the resistance curve resulting from the scaling of the air flow rate is the red-circle curve (Q_{fs}). The percentage differences shown in Fig. 5a are calculated compared to full scale simulations in natural ventilation mode Q_{ns} (black-triangle curve), assumed here as a baseline. Evidently, the ITTC resistance curve is very close to the one related to the natural ventilation Q_{ns}, with a maximum difference of -3.3% at low speed (Fr 0.97).

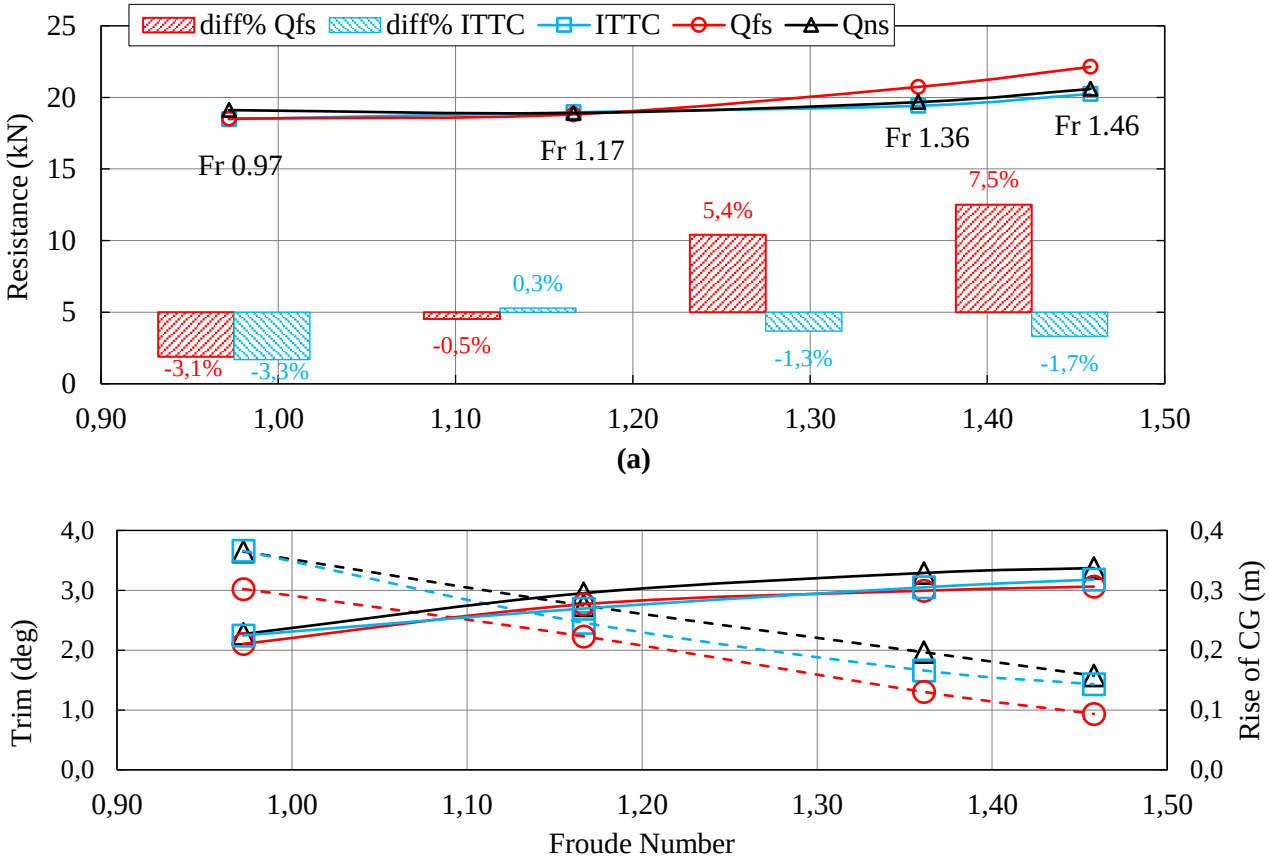

Figure 5. (a) Comparison between resistance curve with ITTC-based scaling and full scale simulations with $\boldsymbol{Q_{ns}}$ and $\boldsymbol{Q_{fs}}$. The differences are relative to $\boldsymbol{Q_{ns}}$.
(b) Trim (dotted curves) and Rise of CG (continuous curves)

At Fr 1.17 there is the minimum difference from Q_{ns} for both the scaling approaches. The case of scaled air flow Q_{fs} shows increasing differences for higher speeds (up to Fr 1.46).

The curves show that the main source of error is due to air flow. The small percentage differences observed for the ITTC curve emphasize the reduce impact of the scale effect due to the different wetted surfaces between the model and ship scales. In essence, the percentage differences between the wetted surfaces shown in Fig. 6 are significantly greater than those related to the resistances shown in Figure 5a (cyan and black curves), thus suggesting that the hypothesis in Eq. 2 is reasonable.

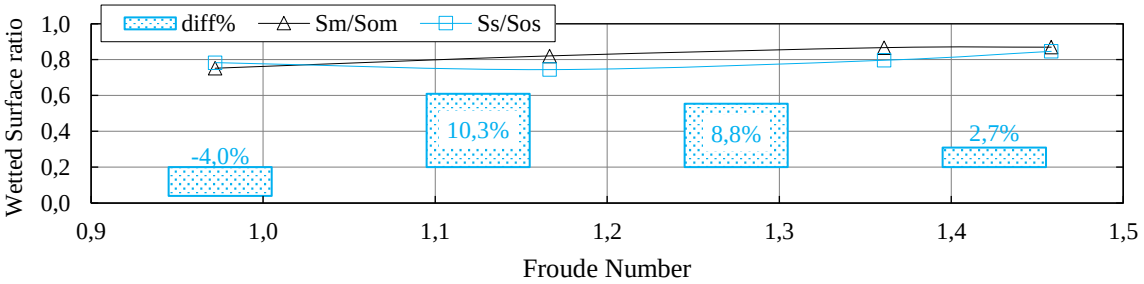

Figure 6. Comparison between full scale and model scale wetted surface reduction.

As Fig.6 shows only the wetted surface ratios, the comparison of the air distribution between model and full scale cases in Fig. 7 show a better picture of the air lubrication technique effects.

As can be observed in Fig. 7, there is little to no difference in the air distribution on the hull bottom downstream of the forward interceptor between model scale and full scale. However, Fig. 7 reported a notable difference in the wetted surface ratio, around 10% to 9% for Fr=1.17 and Fr=1.36 respectively. In this case, the difference in wetted surface is more related to the difference in trim between model and full scale than to the extent of dry patches induced by ventilation. This can be seen clearly in the plot in Fig. 5b (black and cyan curves), which shows that the full scale simulation has higher running trim values, particularly for the two middle hull speeds. This difference can be observed in Fig. 7, where the dynamic waterline for the full scale case starts aft of the model scale case. This leads to a lower wetted surface ratio in full scale, although the wetted surface shape of the ventilated part of the hull remains very similar to the model scale simulation.

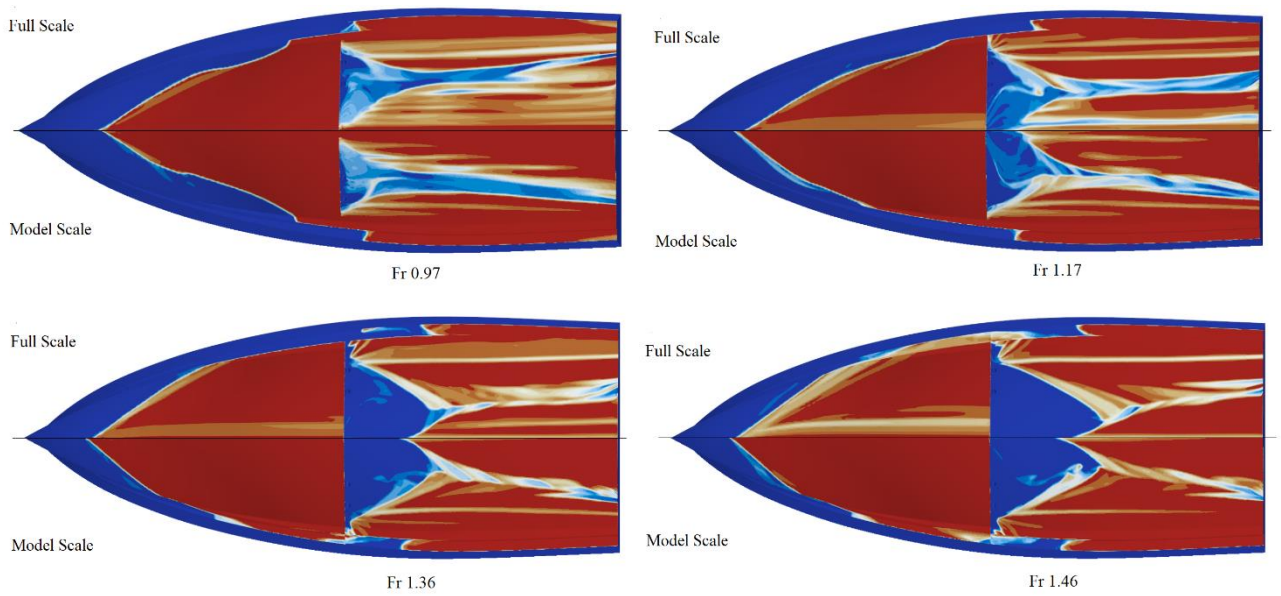

Figure 7. Comparison between model and full scale wetted surface at different Froude numbers with natural ventilation

3.3 Effect of scaling on variable air flow

To analyze the influence of a variable air flow rate in full scale, simulations have been carried out forcing 2 ($2Q_{fs}$) and 5 times ($5Q_{fs}$) the scaled air flow rate (Eq.2). The plots in Fig.8 show the total resistance *vs* Froude Number curves for all the air flow rates in both model and full scale. The reported differences in percentage, shown below the plots, are calculated respect to Q_{nm} and Q_{fs} for model and ship respectively. As observed by De Luca *et al.* (2022), in the model scale (Fig. 8a) an increment of the air flow rate (*e.g.* from Q_{nm} to $2Q_{nm}$) does not necessarily imply a resistance reduction. Conversely (Fig. 8b), the full scale case $2Q_{fs}$ and $5Q_{fs}$ lead to a resistance reduction from Q_{fs}. In particular, the performance improvement appears to be minimal for $2Q_{fs}$, whereas for $5Q_{fs}$, the resistance reduction increases with speed more than in the model scale.

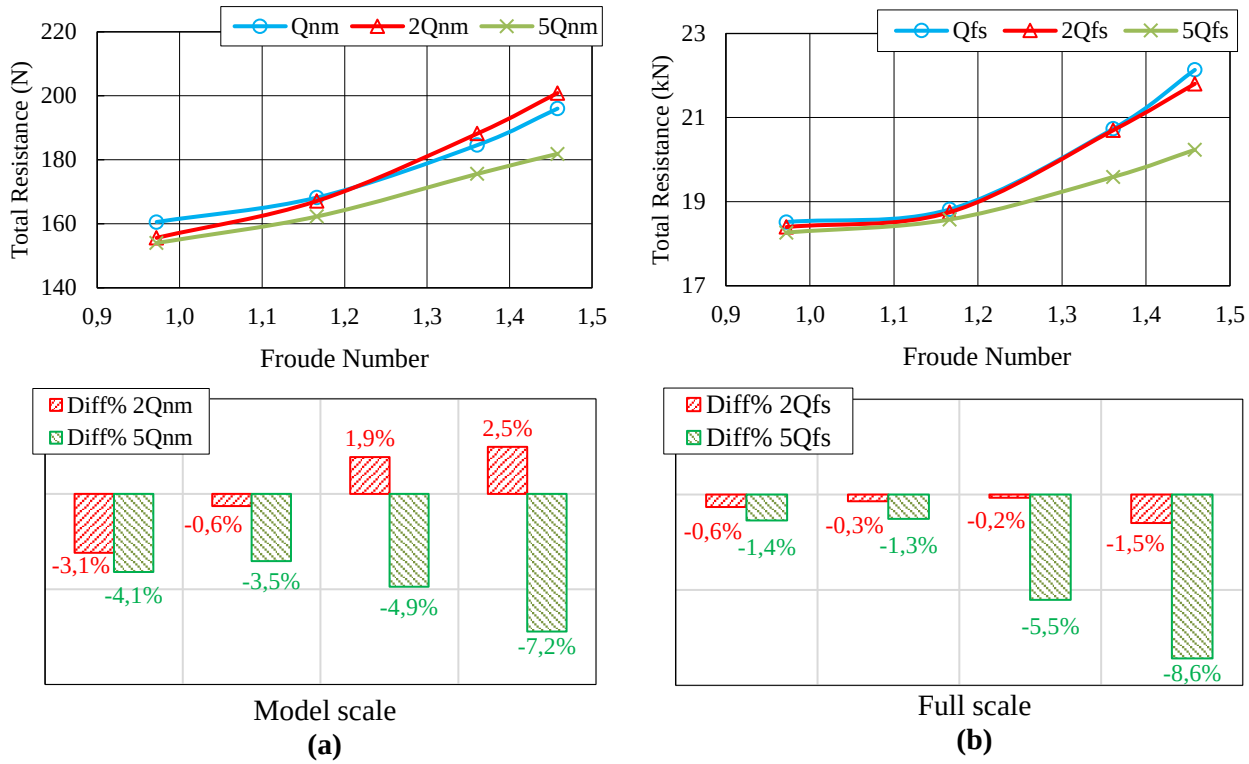

Figure 8. Comparison between model scale resistance with natural ventilation, double and five times the natural ventilation flow rate

4. CONCLUSIONS AND FUTURE WORK

In this work, the study of the application of air lubrication on a DIS-equipped planing hull, with a focus on scaling effects, is presented. In particular, the investigation of the scale effects via CFD simulations has been carried out by taking into consideration three major aspects of the scaling of ventilated planing hulls.

The first deals with the scaling law concerning the actual injected air flow rate used to enhance the AL on the DIS-equipped hull with natural ventilation. The theoretical scaling approach using Froude number similitude for the airflow velocity has been compared with full-scale simulation results. A better scaling law exponent derived from full-scale air flow data is slightly lower than the Froude scaling one. Therefore, the proposed scaling law based on full-scale CFD results allows for a better estimation of full scale air flow for model-ship correlation.

The second aspect is about the total resistance scaling using a hybrid experimental-CFD approach based on ITTC guidelines. We used CFD to evaluate the model, and consequently the ship's wetted surfaces, for the extrapolation of total resistance. The results are then compared to full-scale CFD and show that the maximum error is about 3% for the lowest speed.

The third takes into consideration variable air flow rates and their effect on model and full-scale. Results with two and five times the natural ventilation flow rate show that full-scale gains always increase with increased air flow, as well as hull speed. This is not the case in model scale, where significant gains are only obtained with the highest air flow rate.

Future work on Air Lubrication applied to planing hulls is planned and will include the study of DIS-based air lubrication by doubling the number of injection ports from the current four to eight. The additional injection ports will be placed between the existing ones and the keel line, at the same distance as the forward interceptor.

5. ACKNOWLEDGEMENTS

The PRIN 2017 program, project 2017X7Z8S3 “LUBRI-SMOOTH: Innovative materials and techniques for the reduction of ship resistance", is gratefully acknowledged for the financial support.

REFERENCES

An, H., Pan, H., & Yang, P. (2022). Research Progress of Air Lubrication Drag Reduction Technology for Ships. *Fluids*, *7*(10), 319.

Cucinotta, F., Guglielmino, E., Sfravara, F., (2017). An Experimental Comparison between different Artificial Air Cavity designs for a Planing Hull. *Ocean Engineering*, 140, pp. 233-243.

De Luca, F., & Pensa, C. (2012). Experimental investigation on conventional and unconventional interceptors. *Trans. Int. J. Small Craft Tech*, 154, 65-72.

De Luca, F., Mancini, S., Miranda, S., Pensa, C., 2016, An Extended Verification and Validation Study of CFD Simulations for Planing Hulls, *Journal of Ship Research*, Vol. 60, No. 2, pp. 101–118.

De Luca, F., Mancini, S., Pensa, C., Pigazzini, R., & Sorrentino, V. (2022). A DIS-Based Air Cavity Concept for Planing Hull. In *Technology and Science for the Ships of the Future* (pp. 538-545). IOS Press.

Foeth, E. J. (2008). Decreasing frictional resistance by air lubrication. In *Proceedings of the 20th International HISWA Symposium on Yacht Design and Yacht Construction, Amsterdam, The Netherlands*, 17-18 November 2008, Edited by PW de Heer, ISBN: 978-90-811322-2-0, paper: P2008-8 Proceedings.

Gokcay, S., Insel, M., & Odabasi, A. Y. (2004). Revisiting artificial air cavity concept for high speed craft. *Ocean Engineering*, 31(3-4), 253-267.

Gokcay, S., Insel, M. (2011, March). Utilising air lubrication for energy efficient high speed marine vehicles. In *Proceedings of the Royal Institution of Naval Architects-International Conference: High Speed Marine Vessels, Coventry, UK, 14-15 September 2011*.

ITTC, (2014). Practical Guidelines for Ship CFD Applications. Recommended Procedures and Guidelines 7.5-03-02-03.

ITTC, (2017). High Speed Marine Vehicles Resistance Test. Recommended Procedures and Guidelines 7.5-02-05-01.

ITTC, (2017). Resistance and Propulsion Test and Performance Prediction with Skin Frictional Drag Reduction Techniques. Recommended Procedures and Guidelines 7.5-02-02-03.

Jang, J., Choi, S. H., Ahn, S. M., Kim, B., & Seo, J. S. (2014). Experimental investigation of frictional resistance reduction with air layer on the hull bottom of a ship. *International Journal of Naval Architecture and Ocean Engineering*, 6(2), 363-379.

Kodama, Y., Kakugawa, A., Takahashi, T., Nagaya, S., & Kawamura, T. (2000). Drag reduction of ships by microbubbles. *National Maritime Research Institute of Japan*.

Latorre, R. (1997). Ship hull drag reduction using bottom air injection. *Ocean engineering*, *24*(2), 161-175.

MEPC 1-Circ.1-Circ.815. (2013) Guidance on Treatment of Innovative Energy Efficiency Technologies for Calculation and Verification of the Attained EEDI; International Maritime Organization: London, UK, 2013.

Ricks, A., Morabito, M. G., & Datla, R. (2023). Effect of ventilation on cavity formation on stepped planing hulls. *Journal of Ship Research*, 67(01), 32-47.

Siemens PLM Software, 2021, Star-CCM+ User's Guide 2021.